

LNF - 70/54
Dicembre 1970

D. Schwela: THEORETICAL REPORT ON PION PHOTOPRO-
DUCTION BELOW 1 GeV. -

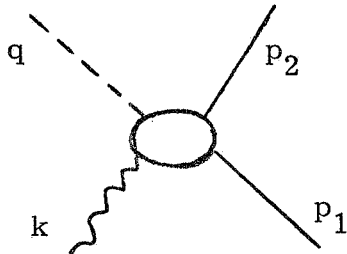
"Frascati Meeting on Electronsynchrotron"
Frascati, November 5-7, 1970

Invited talk, given at the
"Frascati Meeting on Electrosynchrotron"
Frascati, November 5-7, 1970

LNF - 70/54
Dicembre 1970

D. Schwela^(x): THEORETICAL REPORT ON PION PHOTOPRODUCTION BELOW 1 GeV. -

In this talk, our present knowledge on the single pion photoproduction on nucleons for photon energies below 1 GeV will be sketched. This process is symbolized by the diagram



$$s = (k + p_1)^2$$

$$t = (k - q)^2$$

$$u = (k - p_2)^2$$

where k , q , p_1 , p_2 denote the four momenta of photon, pion, ingoing nucleon, outcoming nucleon respectively. s , t and u are the usual Mandelstam variables, constrained by $s + t + u = 2M^2 + m_\pi^2$, M being the nucleon mass, m_π the pion mass.

This talk has three parts: In a first, a short survey of the present status of the theoretical description of this process below 1 GeV will be given. This survey is short since nearly everything of it is already known for two years. In the second part the results of a recent multipole analysis in the first resonance region are discussed. The third part is devoted to the conclusions from this analysis and to suggestions for further experiments.

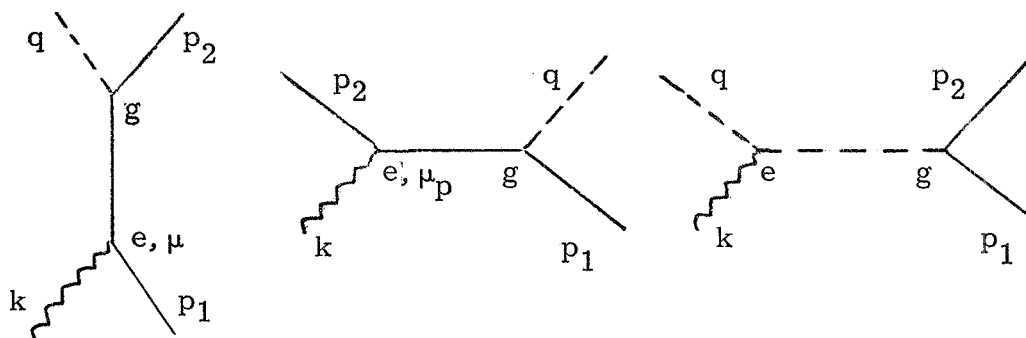
(x) - Physikalisches Institut der Universitaet, Bonn (Germany).

2.

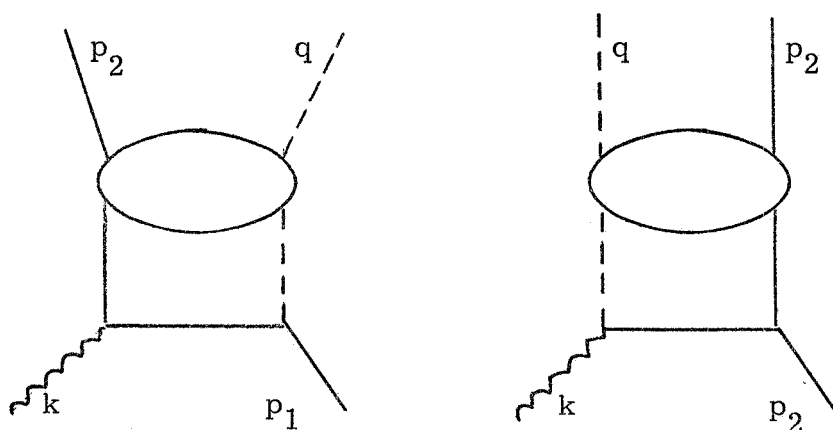
I. - SHORT SURVEY OF THE PRESENT STATUS OF PION PHOTO-
PRODUCTION BETWEEN THRESHOLD AND 1 GeV. -

Since the basic work of Chew, Low, Goldberger and Nambu⁽¹⁾ in 1957 many attempts have been made in order to determine the multi pole amplitudes of pion photoproduction, the most recent, complete and sophisticated ones being those of Berends, Donnachie and Weaver⁽²⁾, Engels and Schmidt⁽³⁾, von Gehlen⁽⁴⁾, Schwela and Weizel^(5, 5a) who used dispersion relations, and those of Kim⁽⁶⁾ and Pfeil⁽⁷⁾ who used the isobar model. The first approach is reliable only for energies below $E_\gamma = 0.5$ GeV, while the second one can be applied in the whole region of resonances.

Every theory of pion photoproduction starts with the calculation of the Born diagrams



where the photon interacts with the charge and the magnetic moment of the nucleon and the charge of the pion. The problem then is to include the strong final state interaction between nucleon and pion as is represented e. g. by the graphs



The main features of the dispersive and isobar approach in solving this problem are as follows :

I.1. - Dispersive approach.

In the dispersive approach one writes down fixed - t - dispersion relations for the twelve invariant photoproduction amplitudes A_i (the index i contains the decomposition into Lorentz-invariants spin

matrices and isotopic spin properties)

$$(1) \quad A_i(s, t) = A_i^{\text{BORN}}(s, t) + \frac{1}{\pi} \int_{(M+m_\pi)^2}^{\infty} ds' \text{Im} A_i(s', t) \left[\frac{1}{s'-s} \pm \frac{1}{s'-u} \right]$$

In this equation, A_i^{BORN} are the invariant amplitudes of the Born graphs and the + or - sign of the second integral depends on the crossing properties of the actual amplitude. Starting from eq. (1) one projects out to partial waves by expanding the amplitudes A_i in terms of multipole amplitudes

$$M_{1\pm}^i(W) \quad \text{and} \quad E_{1\pm}^i(W)$$

which are functions of the total CMS-energy $W = \sqrt{s}$; l is the orbital angular momentum of the pion and the \pm sign indicates whether $y = 1 \pm \frac{1}{2}$; $i = 0, 1/2, 3/2$ denotes the isospin indices, 0 coming from the isoscalar part, and $1/2, 3/2$ coming from the isovector part of the electromagnetic hadron current.

By this projection procedure one obtains a system of dispersion relations for the multipole amplitudes which, for brevity we denote by $M_i = (M_{1\pm}^i, E_{1\pm}^i)$

$$(2) \quad M_i(W) = B_i(W) + \frac{1}{\pi} \int_{M+m_\pi}^{\infty} dW' \frac{\text{Im} M_i(W')}{W'-W-i\epsilon} + \\ + \sum_j \frac{1}{\pi} \int_{M+m_\pi}^{\infty} dW' K_{ij}(W, W') \text{Im} M_j(W')$$

In this equation, $B_i(W)$ denotes the projection of the Born terms and $K_{ij}(W, W')$ are explicitly known, nonsingular kernels. The usefulness of this multipole expansion is due to the Watson⁽⁸⁾ theorem which is a consequence of the unitarity of the S-matrix and the assumption of time reversal invariance of strong and electromagnetic interactions. This theorem relates a multipole of definite angular momentum and isotopic spin with the corresponding pion nucleon amplitude, i. e.

$$(3) \quad M_i = \pm |M_i| e^{i\delta_i}$$

or equivalently

$$(4) \quad \text{Im} M_j = e^{-i\delta_j} \sin \delta_j M_j$$

where δ_i denotes the (real) pion nucleon phase shift.

4.

Several difficulties are connected with (2), (4) :

- 1) The Watson theorem is strictly valid only below the two pi on production threshold. Above this threshold at $E_\gamma = 320$ MeV, eq. (4) is strictly only the definition of the multipole phase.
- 2) The multipole phase has to be known on the whole physical cut.
- 3) The eq. (2) is valid only for small W , a fact which is due to the divergence of the Legendre series expansion of the invariant amplitudes into multipoles. This is connected with the presence of singularities in the t - and u -channels.

While nobody has succeeded in resolving the third difficulty, the first two have been overcome by two mainly different approaches which, of course, are essentially drastic assumptions :

- a) Here one considers only the lowest multipole amplitudes with $l \leq 2$ and

either introduces a cut off in (2) assuming the validity of the Watson theorem up to this cut off (Engels and Schmidt⁽³⁾)

or makes assumptions about the high energy behaviour of the multipole phases doing some educated guesswork (von Gehlen⁽⁴⁾, Schwela and Weizel⁽⁵⁾).

- b) In the approach of Berends et al.⁽²⁾ conformal mapping techniques are applied in order to reduce the system of singular integral equations (2) to a system of linear algebraic equations. This latter system is then formulated and solved using only the experimentally known πN phases.

The main difference between the two approaches a) and b) is the occurrence of free parameters in a). This is due to the fact that for certain assumptions for the high energy behaviour of the multipole phase shift solutions exist for the homogeneous eq. (2), i. e. the equation setting $B_i(W) \equiv 0$. This corresponds to the well known existence of CDD zeroes⁽⁹⁾ in the amplitude. These parameters cannot be determined from the theory, they have to come from "outside" and it seems appropriate to fit them on experimental data.

In contrast to this situation, the solutions of approach b) are unique, which from a theoretical point of view is more satisfactory insofar as absolute predictions are obtained. However, the procedure of ref. (2) is not transparent enough to indicate which solution is chosen out of the larger class of possible ones.

For more details on the approaches a) and b) the reader is referred to the original papers and to the review talks of Rollnik⁽¹⁰⁾ and Weaver⁽¹¹⁾.

In order to give an impression of the quality of these calculations, we compare the results of ref. (2) and ref. (5) which are the most complete and elaborate calculations. In Fig. 1 we have the angular di-

tribution of the differential cross section for $\gamma p \rightarrow p\pi^0$ at $E_\gamma = 320$ MeV, compared to the prediction of ref. (2) (shaded area) and the fit of the data of ref. (5a) which determined the open parameters. As is clearly seen the BDW result lies substantially below the experimental data⁽¹²⁾. On the other hand also the result of ref. (5a) does not represent the small angle data. In Fig. 2 the angular distribution of the differential cross section for $\gamma p \rightarrow n\pi^+$ at $E_\gamma = 340$ MeV is shown. Both predictions agree quite well with the data. In Fig. 3 we have the angular distribution of the differential cross section for $\gamma p \rightarrow p\pi^0$ at $E_\gamma = 180$ MeV. Quite large deviations occur between theoretical results and experiment. The multipole analysis reported in Part II shows that these deviations are due to a too small $M_{1+}^{3/2}$ and a too large $|M_{1-}|$ in case of ref. (2) and to an incorrect $E_{0+}^{\pi^0}$ and a too large $|M_{1-}|$ in case of ref. (5a). In Fig. 4 the excitation curve for the asymmetry ratio $\Sigma(90^\circ)$ for $\gamma p \rightarrow p\pi^0$ is presented. It should be noted that both theories predict too low values at energies below the first resonance. It will be seen in the next Part that this failure is due to the fact the $|M_{1-}^{1/2}|$ as predicted by these theories is too large.

The same quantity for $\gamma p \rightarrow n\pi^+$ is displayed in Fig. 5, which exhibits general agreement. The recoil proton polarization for $\gamma p \rightarrow p\pi^0$ is shown in some angular distributions in Fig. 6. For this quantity both theories give the same predictions so only one curve is drawn. Apart from a completely different slope of data at $E_\gamma = 300$ MeV, there is agreement between theory and experiment except at large pion CM angles, this being due again to the large $M_{1-}^{3/2}$ prediction.

In Fig. 7 the angular distribution for the differential cross section for $\gamma n \rightarrow p\pi^-$ is shown. For ref. (5, 5a) this process involves two more free parameters (see the footnote after ref. (5a)) which have been determined from the differential cross section data of refs. (13, 20, 21, 25, 26). The agreement is good for both theories, although at large backward angles the prediction of ref. (2) turns out to be too high, which is even more exhibited at larger energies. To round the picture, Fig. 8 displays the asymmetry ratio $\Sigma(90^\circ)$ for polarized photons for $\gamma n \rightarrow p\pi^-$. Agreement is somewhat better for refs. (5a, 28) than for ref. (2), except for the data of ref. (24) which, however, seem a little bit too low, compared to those of ref. (23).

Summarizing this discussion we state:

The dispersive approach accounts well for the main features of single pion photoproduction. However, also the neatest description^(5a) does not account for the

differential cross sections for $\gamma p \rightarrow p\pi^0$ at $\theta_{CM} \approx 80^\circ$, $E_\gamma \approx 340$ MeV
differential cross sections for $\gamma p \rightarrow p\pi^0$ in the near threshold region
differential cross sections for $\gamma p \rightarrow n\pi^+$ above $E_\gamma = 380$ MeV
asymmetry ratio $\Sigma(90^\circ)$ below $E_\gamma = 300$ MeV.

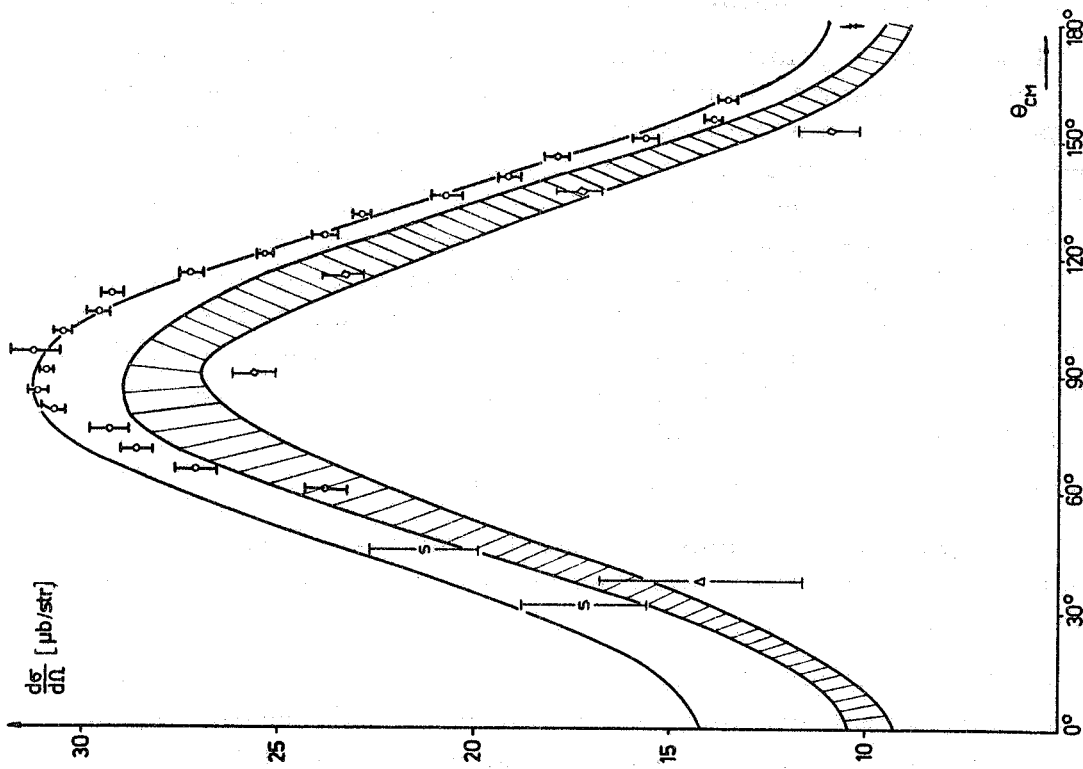


FIG. 1 - Angular distribution of differential cross section for $\gamma p \rightarrow p\gamma^0$ at $E_\gamma = 320$ MeV. Data are from refs. (12, 13).

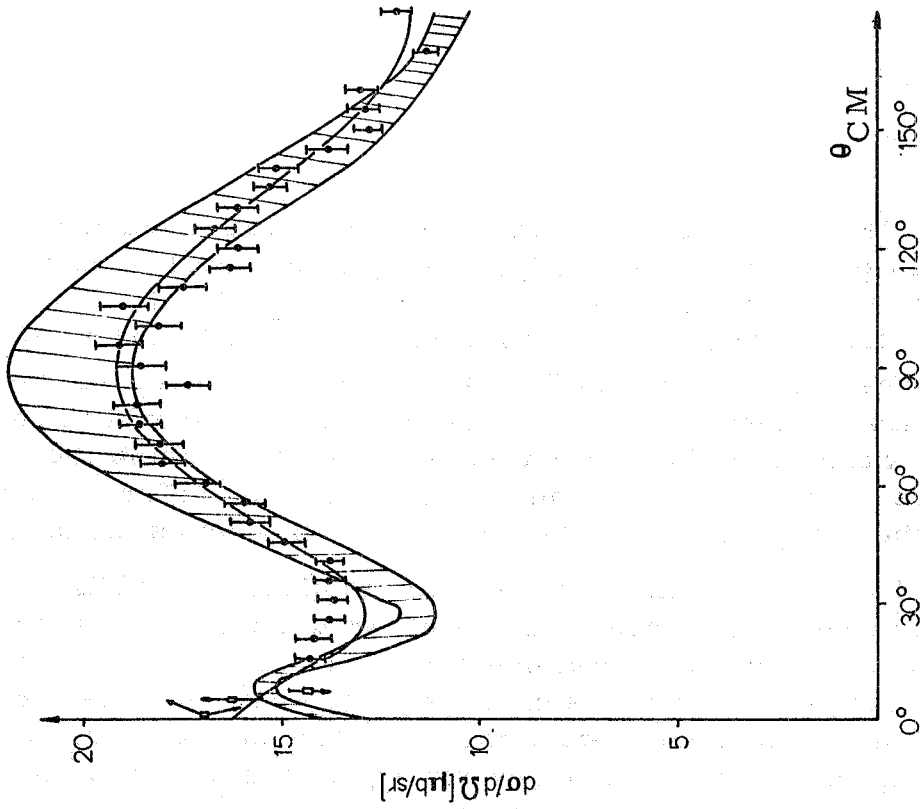


FIG. 2 - Angular distribution of differential cross section for $\gamma p \rightarrow n\pi^+$ at $E_\gamma = 340$ MeV. Data are from refs. (12, 14).

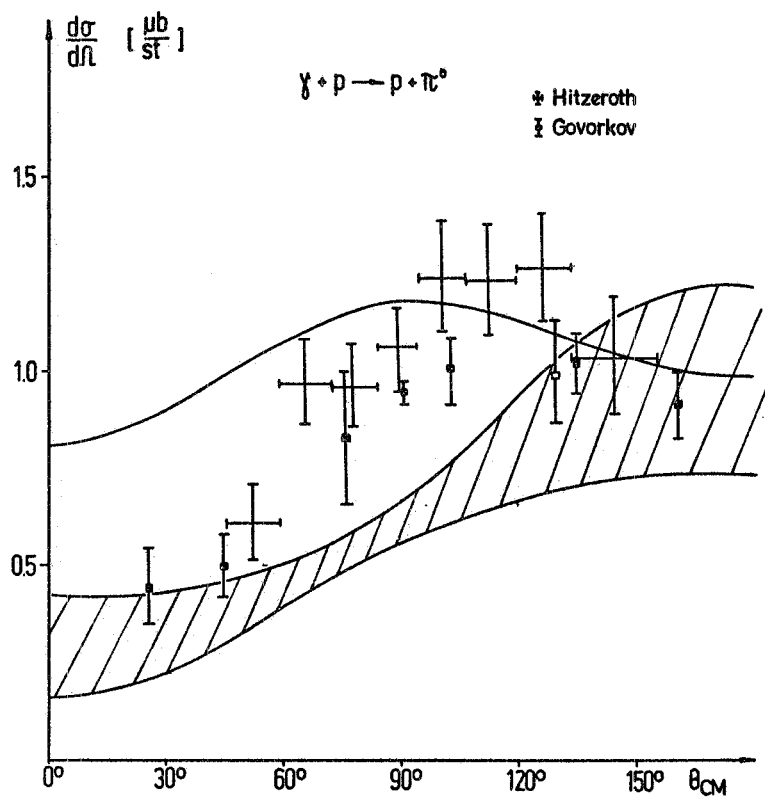


FIG. 3 - Same as Fig. 1 at $E_\gamma = 180$ MeV.
Data are from refs. (15, 16).

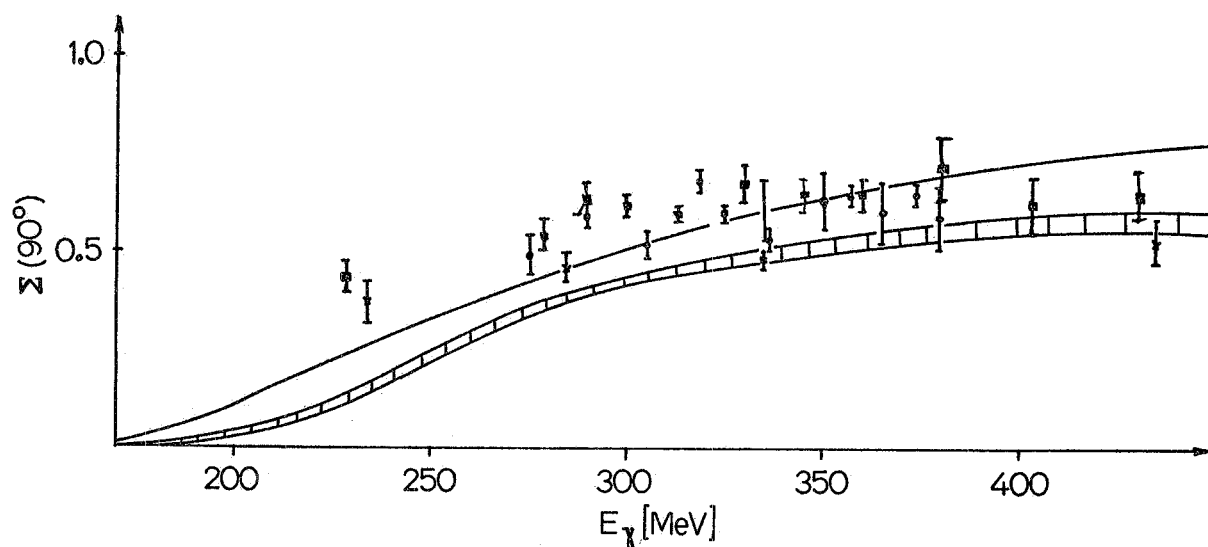


FIG. 4 - Excitation curve for the asymmetry ratio $\Sigma(90^\circ)$ for $\gamma p \rightarrow p\pi^0$.
Data are from ref. (17).

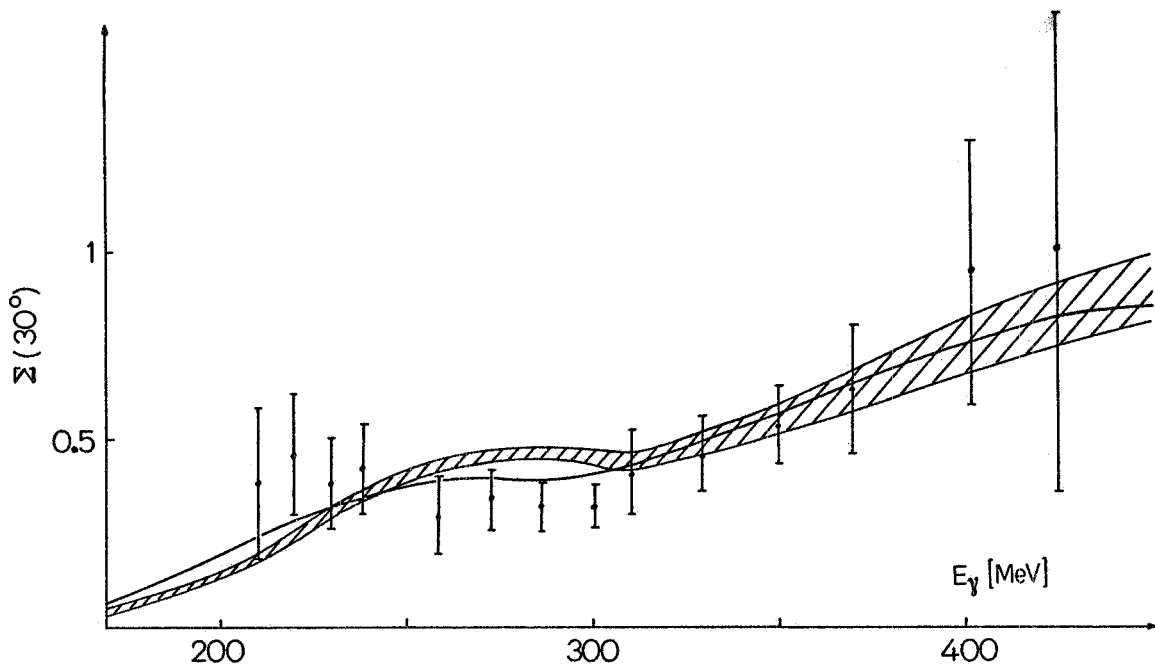


FIG. 5 - Same as Fig. 4 for $\gamma p \rightarrow n\pi^+$. Data are from ref. (27).

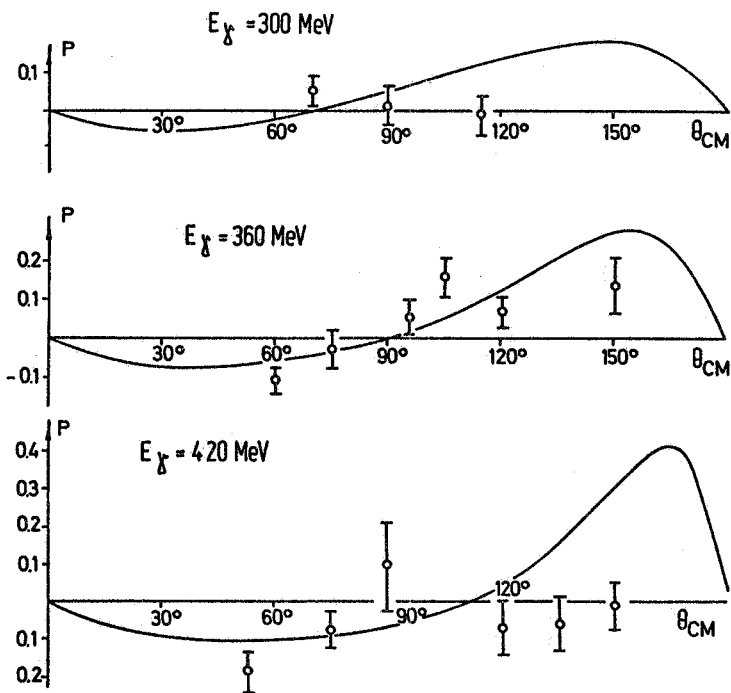


FIG. 6 - Angular distributions for recoil proton polarizations at $E_\gamma = 300, 360, 420$ MeV for $\gamma p \rightarrow p\pi^0$. Data are from ref. (18).

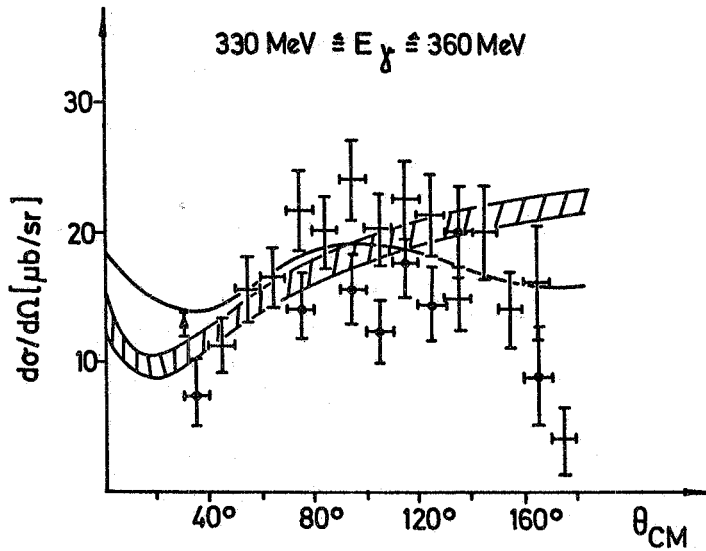


FIG. 7 - Angular distributions for differential cross section for $\gamma n \rightarrow p\pi^-$ at $E_\gamma = 340$ MeV. Data are from refs. (1a, 21, 22).

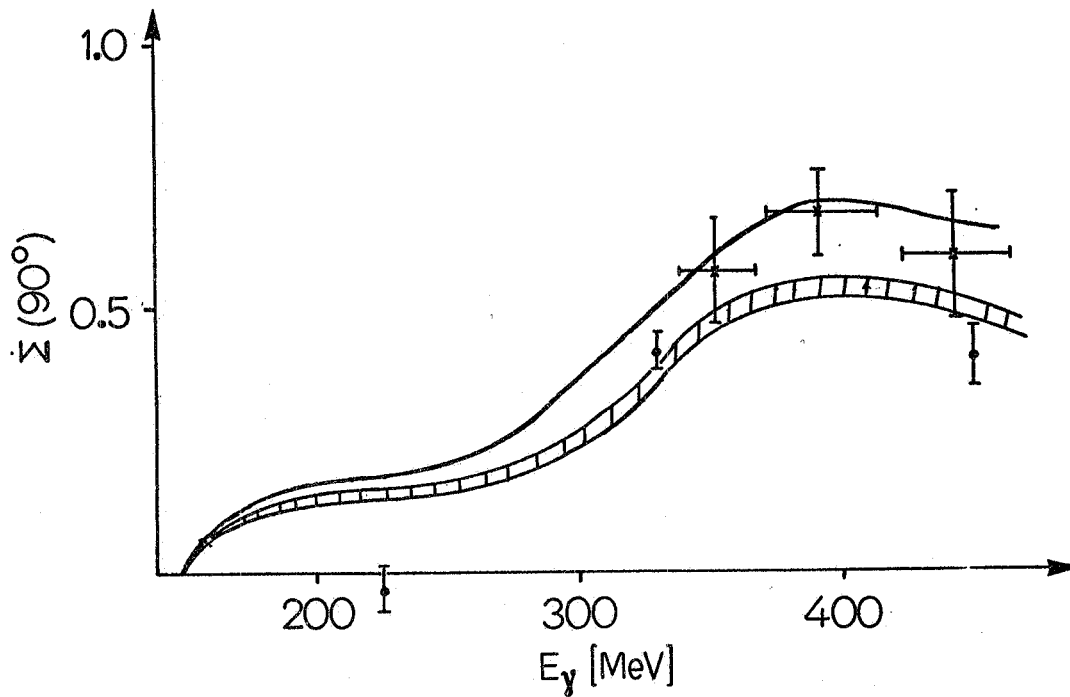
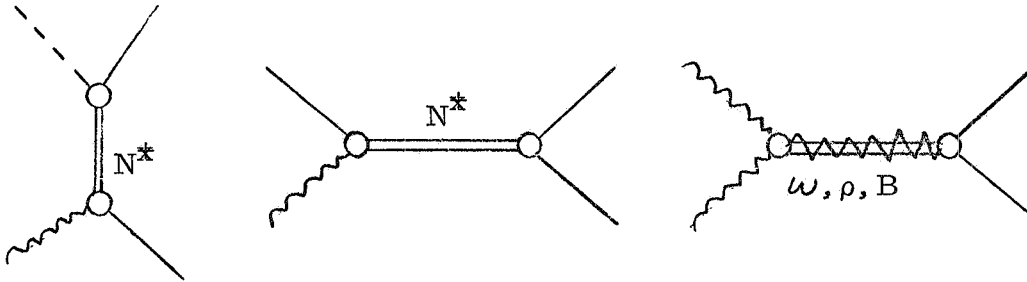


FIG. 8 - Asymmetry ratio $\Sigma(90^\circ)$ for $\gamma n \rightarrow p\pi^-$. Data are from refs. (23, 24).

I.2. - The isobar model.

The isobar model has been applied to photoproduction of pions first by Gourdin and Salin⁽²⁹⁾. It has been refined and extended in the last few years by several people^(30, 6, 7), the most complete and elaborate calculations being those of Pfeil⁽⁷⁾ and Kim⁽⁶⁾ at Bonn.

In the isobar model one calculates - using quantum field theoretical methods - the contribution of the Feynman diagrams



then any invariant amplitude is written,

$$(5) \quad A(s, t) = A^{\text{BORN}}(s, t) + \sum_{N^*} \left[\text{diagram 1} + \text{diagram 2} \right] + (\rho, \omega, B) - \text{exchange}$$

where the sum runs over all allowed states^(o). In practice, one starts by considering the nucleon resonances as stable particles with definite spin and real masses M^* and defines effective Hamiltonian interactions for the various vertices. However, the field theoretic description contains many sources of trouble as no satisfactory free field theory for spin $\geq 3/2$ particles is known. This boils down to the fact that the propagator of the intermediate particles with spin $\geq 3/2$ cannot be determined uniquely. In order to circumvent these troubles a pole approximation for the invariant amplitudes is made,

$$(6) \quad A(s, t) = \frac{a(s = M^{*2}, t)}{s - M^{*2} + i M^* \Gamma(s)} + u \text{ channel}$$

where we have already generalized the ansatz to unstable particles of finite width $\Gamma(s)$. In addition to overcome the propagator ambiguity the pole approximation guarantees an acceptable high energy behaviour of $A(s, t)$. In $a(s = M^{*2}, t)$ the coupling constants of the vertex functions enter as free parameters to be determined by experiment.

Strictly speaking, the assumptions made can only be justified by the success of the model in representing the data in a satisfactory

(o) - Of course from the point of view of duality arguments the isobar model involves double counting if t-channel exchanges are included additively.

way. To illustrate that this is really the case, in Figs. 9-14, the results of the calculations of refs. (6, 7) for π^0 and π^+ photoproduction quantities is shown. The solid line is a fit to the π^0 and π^+ differential cross section data with the seven isobars $P_{33}(1230)$, $P_{11}(1470)$, $D_{13}(1520)$, $S_{31}(1670)$, $F_{15}(1690)$, $D_{15}(1680)$ and $S_{11}(1710)$ exchanged in the s- and u-channel.

In Fig. 11 which shows all existing data for $d\sigma/d\Omega(\gamma p \rightarrow p\pi^0)$ at 180° , only the data of ref. (31) have been included in the fit. (From this picture it seems absolutely necessary to reduce the discrepancies between the results of different laboratories).

The isobar model in the formulation presented gives a satisfactory representation of the present experimental differential cross section data of π^0 and π^+ photoproduction in the energy range from three hold to 1.2 GeV. Even the asymmetry ratios in the whole energy range and the recoil nucleon polarization above $E_\gamma = 500$ MeV are well described, although these data are not included in the fit of the parameters. Some discrepancies are present for the π^+ differential cross section and the proton polarization for $\gamma p \rightarrow p\pi^0$ in the first resonance region. These discrepancies are correlated with the fact that the Watson theorem is badly violated for the nonresonant multipole amplitudes which play an appreciable role in these quantities through interference terms.

For this reason, the dispersive calculations are superior to the isobar model in the first resonance region. Above $E_\gamma = 500$ MeV, however, the sophisticated isobar model is the only model now available which deserves the name of a theoretical model.

Summarizing the results of the approaches I. 1 and I. 2 in the region of the first resonance, we observe :

All theoretical work has confirmed the essential results of CGLN⁽¹⁾, i. e. the predominance of $M_{1+}^{3/2}$ and $E_{0+}^{\pi^+} \approx E_{0+}^{\pi^+} \text{BORN}$.

The calculations of the last few years have been undertaken mainly in order to determine the small multipoles

$$(7) \quad E_{0+}^{\pi^0}, \quad E_{1+}, \quad M_{1-}, \quad \text{and} \quad M_{1+}^{1/2}$$

quantitatively. However, in view of the discrepancies observed between theoretical and experimental results and in view of the fact that different theoretical approaches yield vastly different multipole amplitudes (7), we have to admit: in spite of the elaborate and sophisticated calculations we do not know these multipoles more reliably than CGLN did! Thus, to overcome this unpleasant situation, a striking new idea is needed!

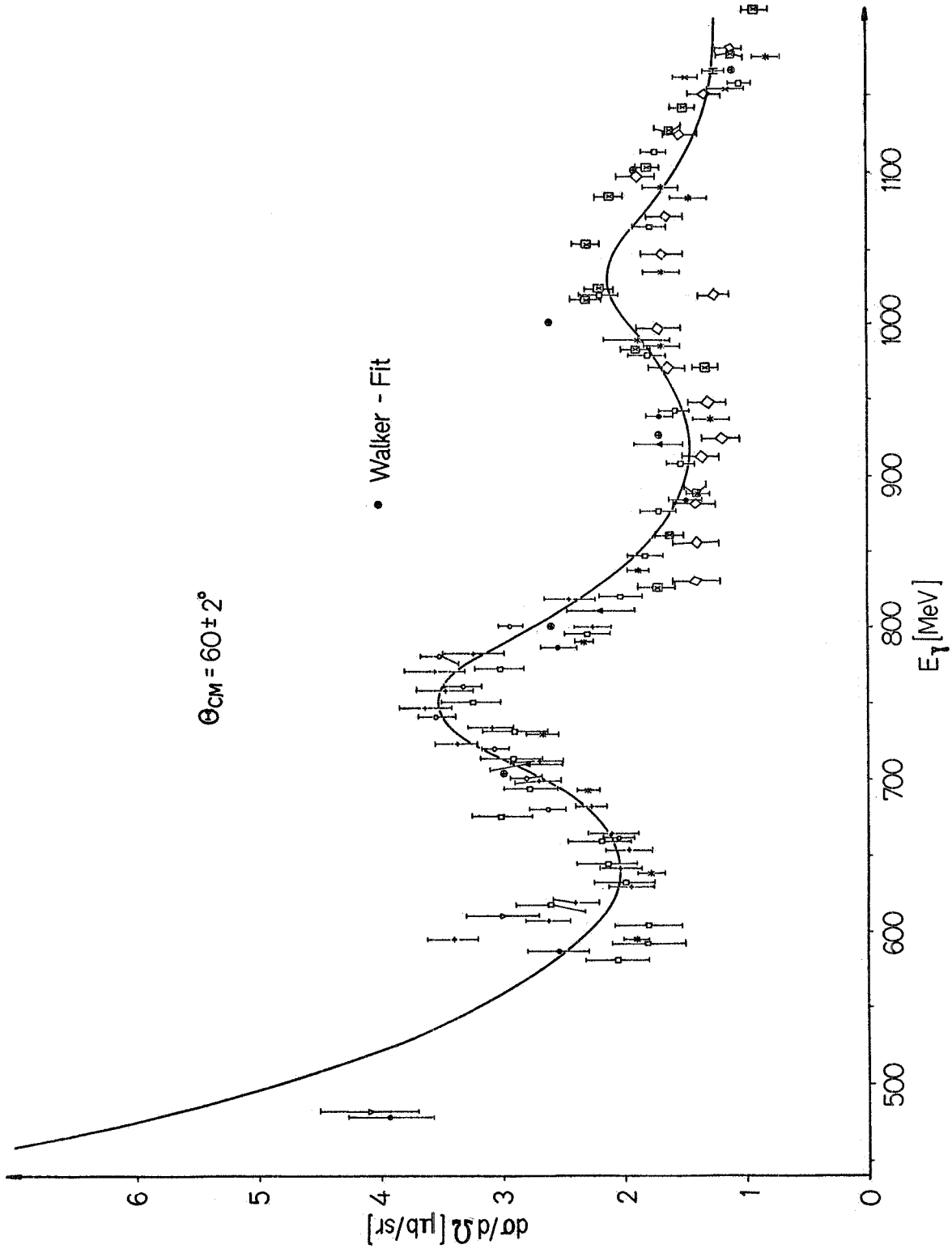


FIG. 9 - Excitation curve for differential cross sections at $\theta = 60^\circ$ for $\gamma p \rightarrow p\pi^0$. For data see refs. (13, 18).

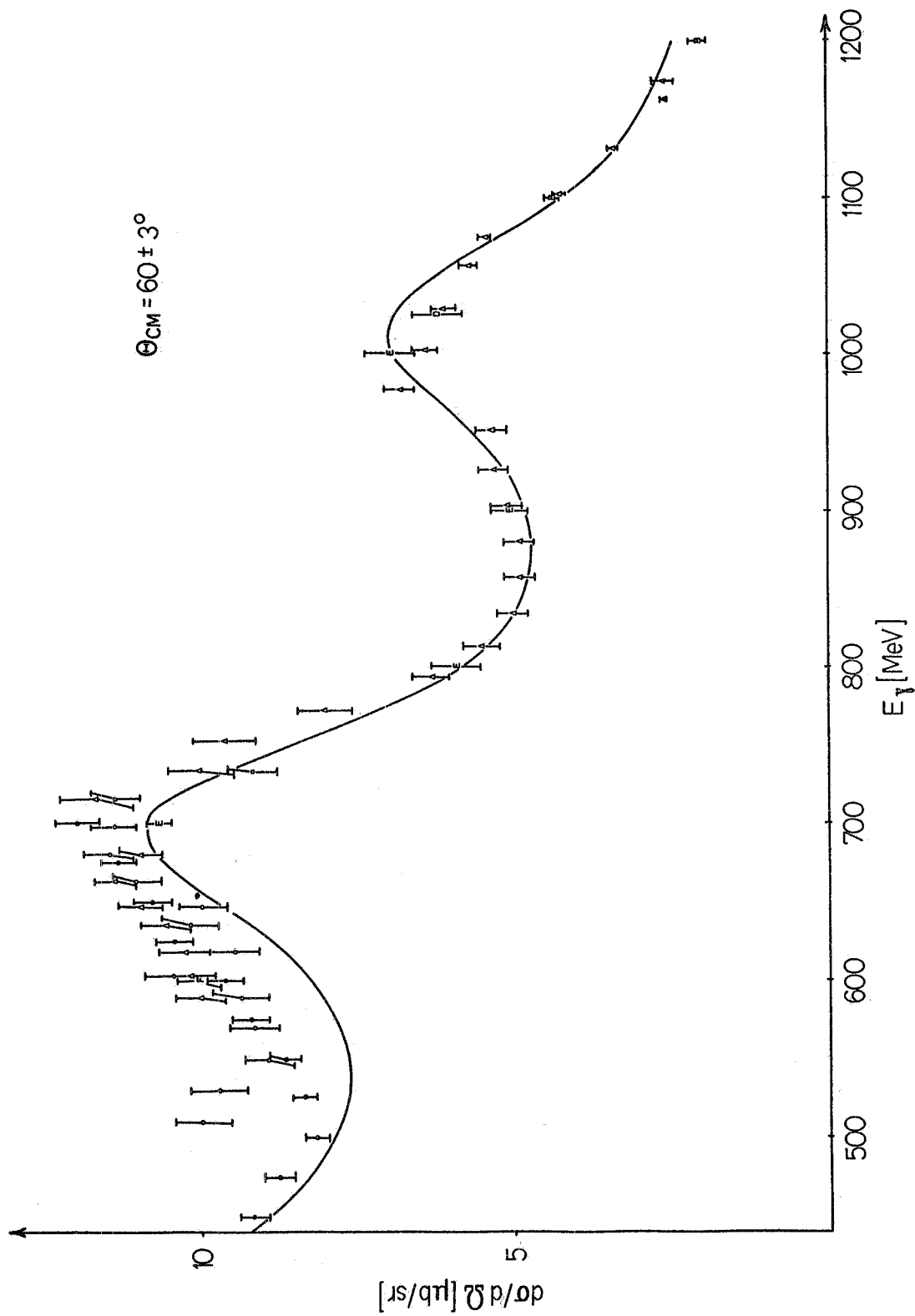


FIG. 10 - Excitation curve for differential cross sections at $\theta = 60^\circ$ for $\gamma p \rightarrow n\pi^+$. For data see refs. (13, 18).

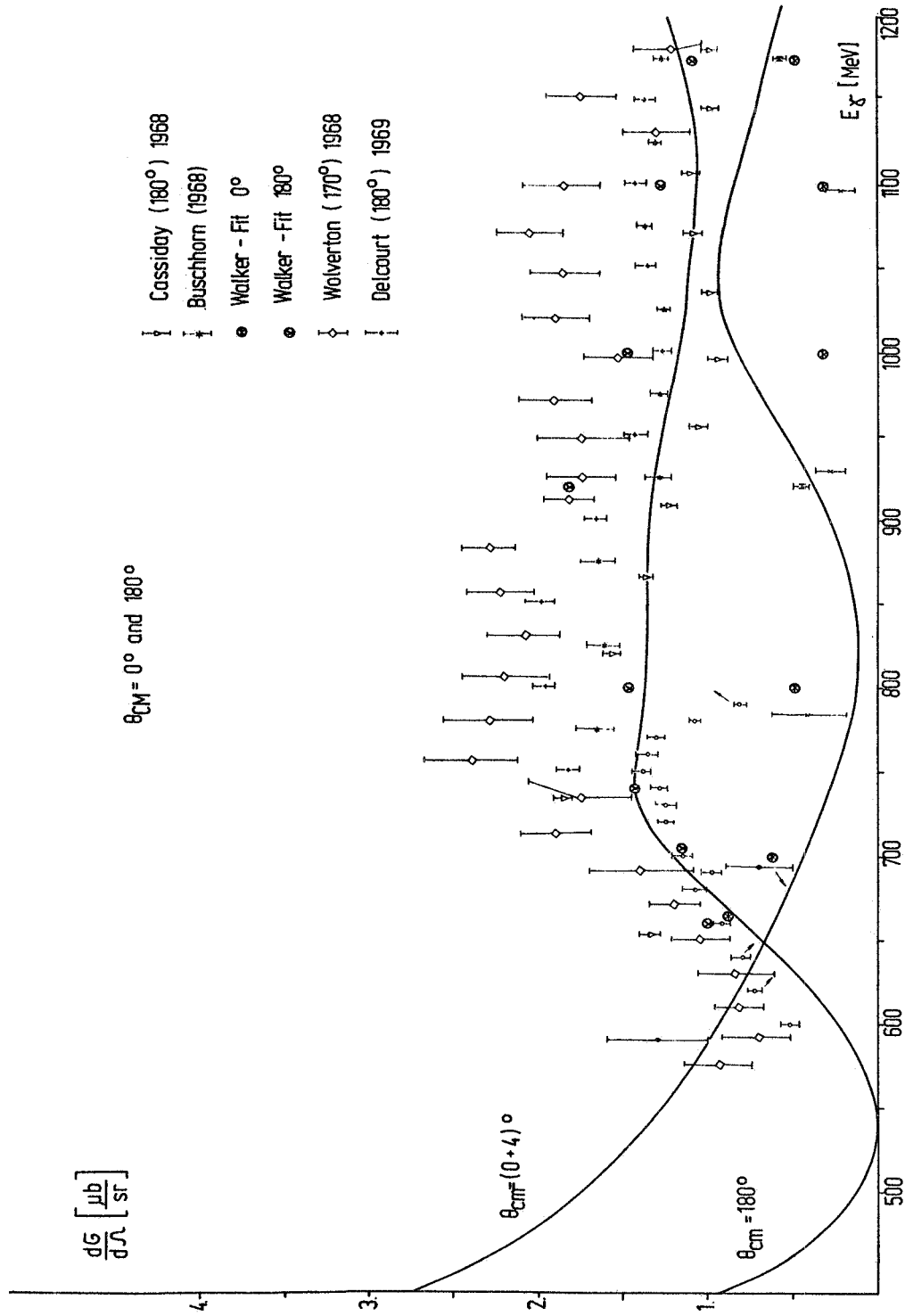


FIG. 11 - Excitation curves for differential cross sections at $\theta = 0^\circ$ and $\theta = 180^\circ$ for $\gamma p \rightarrow p\pi^0$. Data are quoted from ref. (18). Only the Stanford data(31), \mathcal{J} , have been included in the fit.

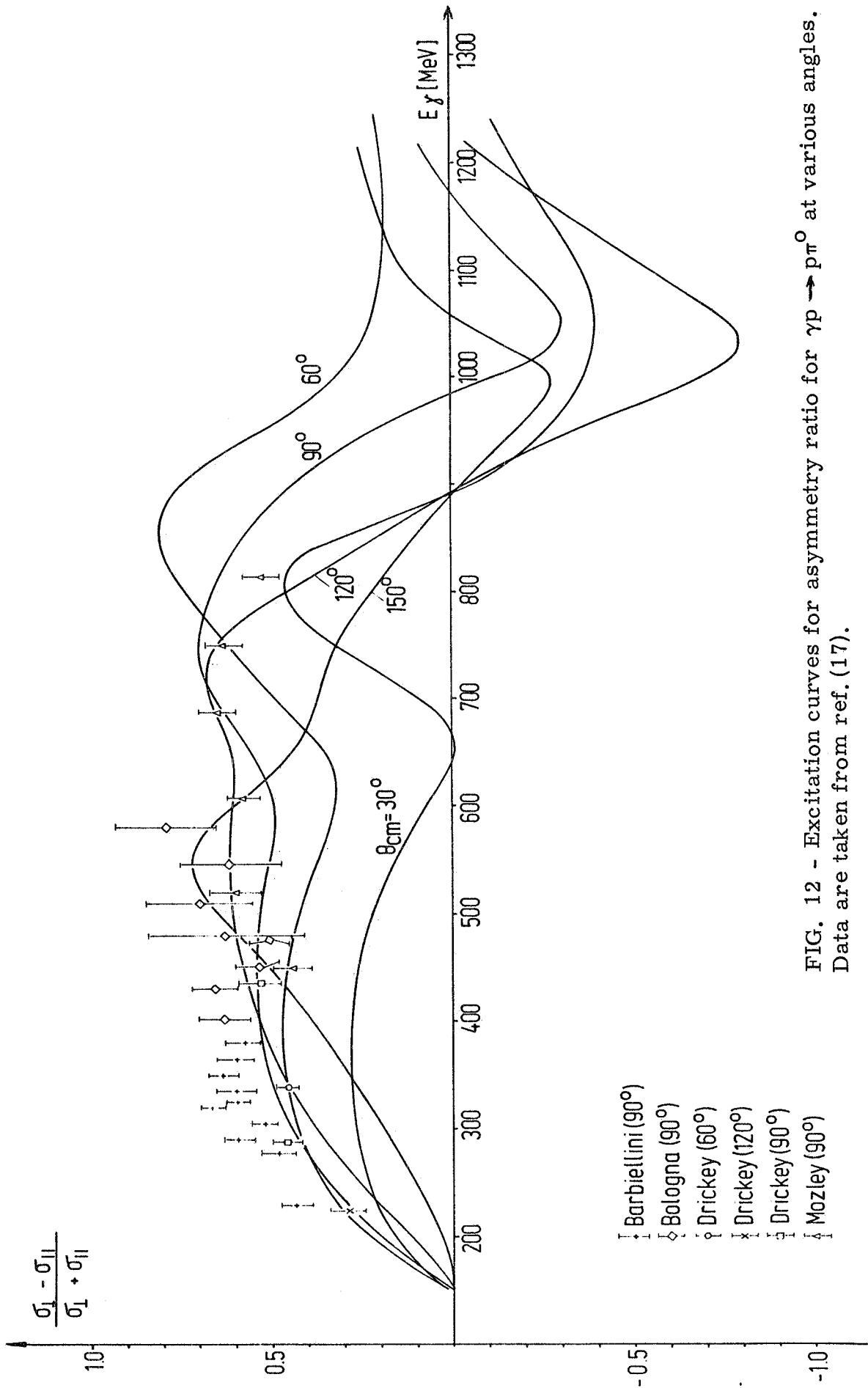


FIG. 12 - Excitation curves for asymmetry ratio for $\gamma p \rightarrow p\pi^0$ at various angles. Data are taken from ref. (17).

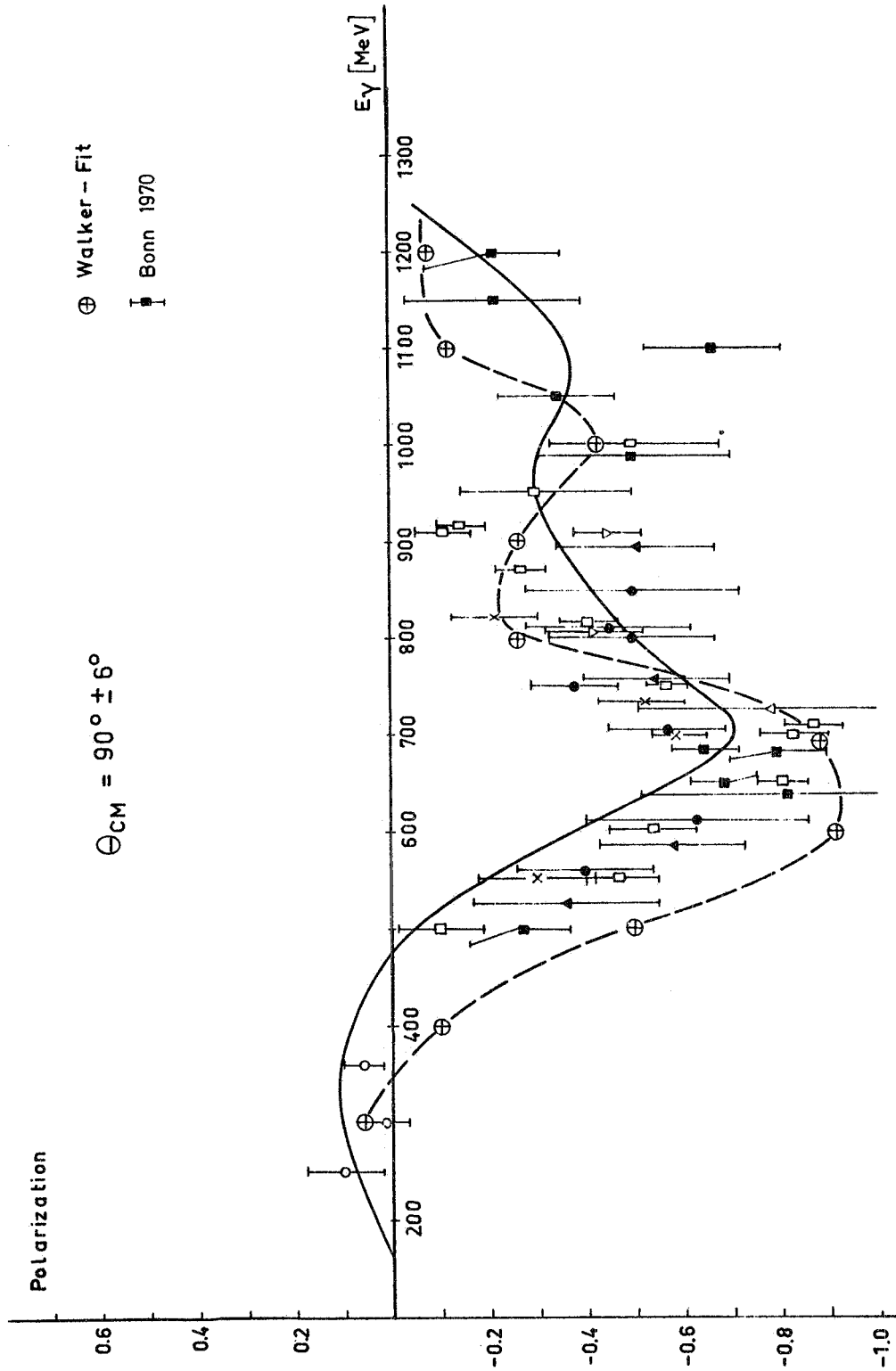


FIG. 13 - Excitation curve of proton recoil polarization for $\gamma p \rightarrow p\pi^0$. Data are quoted from ref. (18).

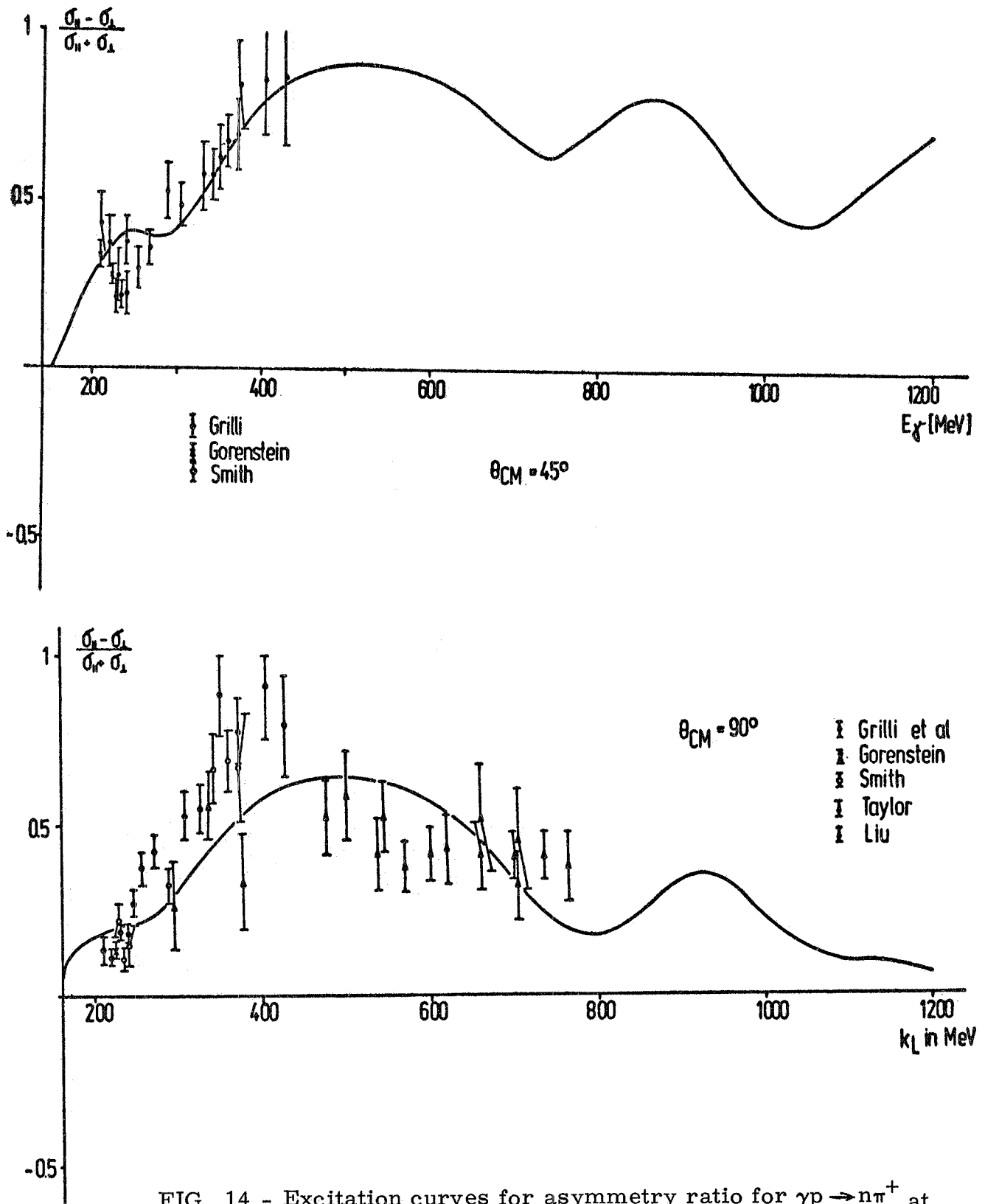


FIG. 14 - Excitation curves for asymmetry ratio for $\gamma p \rightarrow n\pi^+$ at $\theta_{CM} = 45^\circ$ and $\theta_{CM} = 90^\circ$. Data are taken from refs. (27, 13).

II. - RESULTS OF A MULTIPOLE ANALYSIS OF π^0 AND π^+ PHOTO- PRODUCTION BELOW $E_\gamma = 500$ MeV. -

Up to now, nobody has had a striking new idea how to evaluate the small multipoles more reliably. Therefore it seems appropriate, to investigate which of the amplitudes is responsible for the discrepancies one observes between theory and experiment. This has been done very recently by an energy independent multipole analysis, made by P. Noelle, W. Pfeil and D. Schwela⁽³²⁾. "Energy independent" means, that one parametrizes some quantities (i. e. multipole amplitudes) at each energy and tries to fit the experimental angular distributions of all experimental quantities observed at each energy.

Attempts at this goal have been made in the past few years by several people :

Berends and Donnachie ⁽³³⁾ ,	R. L. Walker ⁽³⁴⁾ ,
Grilli et al. ⁽³⁵⁾ ,	Spillantini et al. ⁽³⁶⁾ ,
Aleksandrov et al. ⁽³⁷⁾ ,	Müllensiefen ⁽³⁸⁾ ,
Wennström ⁽³⁹⁾ ,	Kondo et al. ⁽⁴⁰⁾ .

However, the results are not very persuasive, as these analyses are either restricted to a single process^(35, 36, 37, 38) or depend strongly on the assumptions made for some multipoles^(33, 34, 39, 40) which had to be made because of lack of accurate data, and which are not on a sure footing. This situation has become much better with the advent of the new and accurate data of Bonn^(12a, 14a) and Orsay^(12b, 14b) which do allow a more sensitive analysis with a minimum number of assumptions made.

The method of the analysis, the input data and the fit procedure are described in detail in ref. (32), to which the interested reader is referred. The four multipole amplitudes

$$E_{0+}(W), \quad M_{1-}(W), \quad E_{1+}(W) \quad \text{and} \quad M_{1+}(W)$$

have been extracted from the data for $\gamma p \rightarrow p\pi^0$ and $\gamma p \rightarrow n\pi^+$ for 19 energies between $E_\gamma = 180$ MeV and $E_\gamma = 500$ MeV.

The ($l \geq 2$) multipoles have been taken in Born approximation, and the Watson theorem has been used for the $l \leq 2$ multipoles.

When trying a multipole analysis of pion photoproduction in the region of the first pion nucleon resonance, one has to be aware of the fact, that in this energy region photoproduction is largely determined by the magnetic dipole $M_{1+}^{3/2}$. For this reason it is particularly difficult to fix the small multipoles at those energies where $\Sigma(\theta)$ or $P(\theta)$ are not present or not sufficient. At these energies, therefore, one has to expect several possible solutions. Moreover, in the immediate resonance region, the errors of the multipoles will turn out to be large. This can be seen by looking at the asymmetry ratio for polarized photons for $\gamma p \rightarrow p\pi^0$ at $\theta_{CM}^\pi = 90^\circ$. Keeping only interference

terms with M_{1+} , one has :

$$(7) \quad \Sigma(90^\circ) = \frac{\frac{3}{2} |M_{1+}|^2 + \text{Re} \left\{ M_{1+}^* (3 M_{1-} + 3 E_{1+}) \right\}}{\frac{5}{2} |M_{1+}|^2 + \text{Re} \left\{ M_{1+}^* (M_{1-} - 3 E_{1+}) \right\}}$$

If $\Sigma(90^\circ) = 0.6$, as is experimentally the case, near resonance, it is determined practically by the first term in numerator and denominator of eq. (7), and the much smaller rest is not well fixed.

In the beginning of the analysis, at each energy quite a lot of possible solutions were found, except at $E_\gamma = 360$ MeV, where only one solution was obtained, this fact being due to the existence of a complete angular distribution of the recoil proton polarization $P(\theta)$ for $\gamma p \rightarrow p\pi^0$. However,

- 1) by requiring that a continuous connection should exist between adjacent energies, covering the whole energy region;
- 2) by looking at the detailed values for the polarization $P(\theta)$ and the asymmetry $\Xi(\theta)$ and not only at an overall χ^2 value

these solutions were reduced to two sets of multipoles, solution A and solution B.

These solutions are best characterised by the magnetic dipole $M_{1+}^{3/2}$. In Fig. 15A the Argand plot of solution A for this multipole is displayed. All values lie remarkably well on a circle, which, as should be stressed, is not put in by the Watson theorem. In Fig. 15B the Argand plot of solution B is shown (squares).

Clearly the Argand circle is deformed. It should be stressed that solution B fits the experimental data as satisfactorily as solution A does. Only a measurement of the polarized target quantity (up-down asymmetry)

$$(8) \quad \Xi(\theta) = \frac{\frac{d\sigma^\uparrow}{d\Omega} - \frac{d\sigma^\downarrow}{d\Omega}}{2 \frac{d\sigma}{d\Omega}}$$

for π^0 and π^+ production at small pion CM angles and below resonance could decide between solution A and B, as is shown in Table I.

TABLE I

E_γ (MeV)	Solution:	$\gamma p \rightarrow p\pi^0$		$\gamma p \rightarrow n\pi^+$		
		A	B	A	B	
240		35.1	24	27.2	14.1	
260		32.9	17.6	40.8	20.7	
280		14.8	9.8	56.4	29.2	%
300		12.9	3.1	71.1	49.1	

Prediction for $\Xi(60^\circ)$ at various energies for solution A and B.

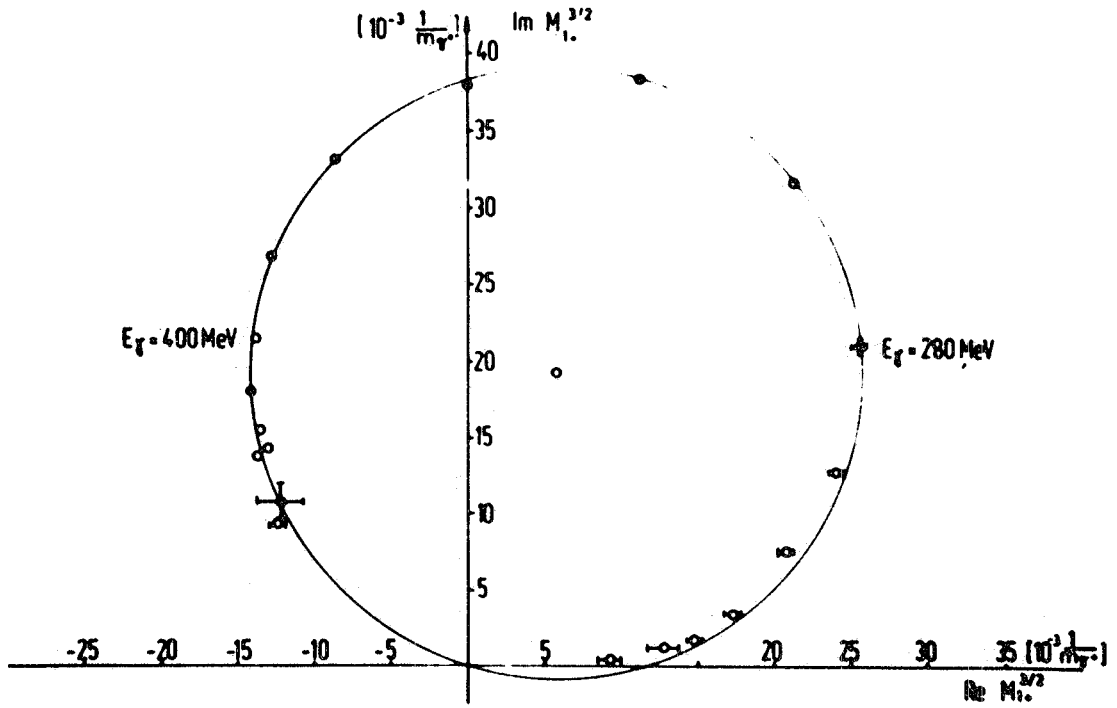


FIG. 15A - Argand plot for $M_{1+}^{3/2}$, solution A.

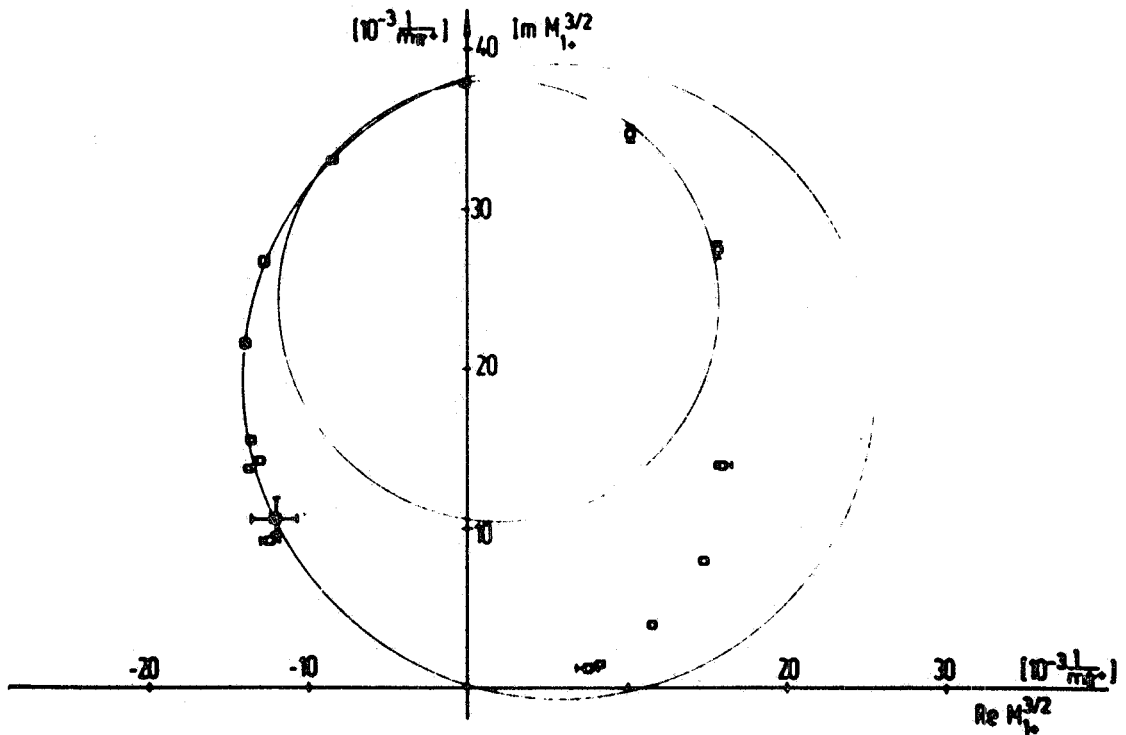


FIG. 15B - Argand plot for $M_{1+}^{3/2}$, solution B, compared to solution A.

The theoretical explanation of the plot of Fig. 15B as a $\Delta(J^P = \frac{3}{2}^+, I = \frac{3}{2})$ resonance is difficult as the total width of the resonance appears to be $\Gamma_{\text{tot}}^B = 70$ MeV, while from solution A $\Gamma_{\text{tot}}^A = 110$ MeV as expected from πN scattering.

Therefore, in the following only solution A is discussed.

In Fig. 16 the theoretical results for $M_{1+}^{3/2}$ are given in an Argand plot, to be compared to the result of the fit, Fig. 15B. To be precise, the circles drawn are adapted to the theoretical curves which below and above the resonance region show some minor deviations from the circle (which, of course, are largest in the threshold region).

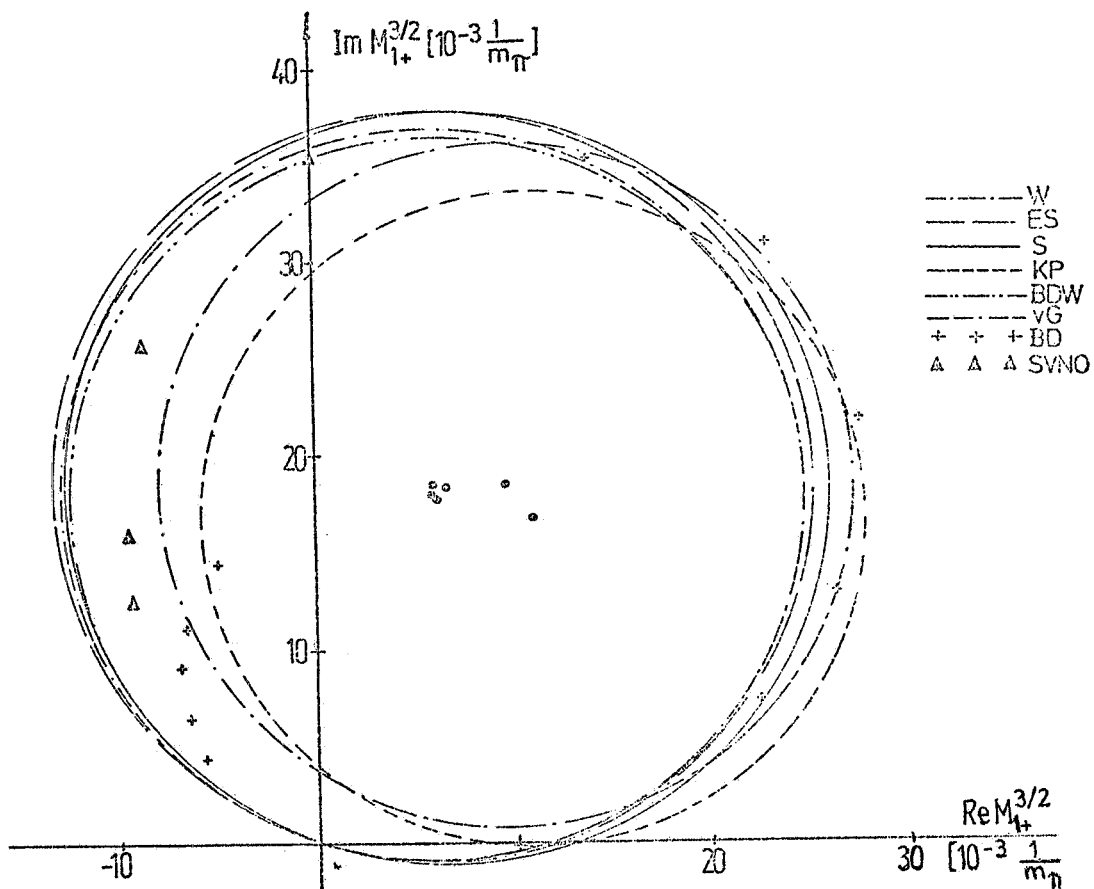


FIG. 16 - The results for $M_{1+}^{3/2}$ from dispersive calculations (2, 3, 4, 5a), isobar model (6, 7) and various phenomenological analyses (33, 34, 36).

The comparison of Fig. 15A and Fig. 16 shows discrepancies of approximately 10% between our result and the results of dispersion theoretic calculations (2, 3, 4, 5a). These deviations have to be considered as large on the scale of the magnitude of $M_{1+}^{3/2}$! The circle of the isobar model calculations (6, 7) and that of Walker's analysis (34) deviate to some greater extent. This might be due to the fact that in these calculations the Watson theorem is violated. The result of the

SVNO analysis which coincides below resonance essentially with the result of BDW⁽²⁾ exhibits also some discrepancies to the fit result, but still is of Breit-Wigner type. In contrast to this really strong differences exist between Fig. 15A and the result of the analysis of Berends and Donnachie, which seems to indicate large deviations from a Breit-Wigner shape for the magnetic dipole amplitude in photoproduction (crossed in Fig. 16).

In Fig. 17 the result of the analysis for the magnetic dipole M_{1-} is presented. In the two amplitudes the errors are quite large. Accurate measurements of angular distributions of the asymmetry ratio $\Sigma(\theta)$ for $\gamma p \rightarrow p\pi^0$ would substantially reduce these errors.

Comparing Fig. 17 to the results of previous calculations in Fig. 18, we observe: While for $\text{Re}(M_{1-}^0 + 1/3 M_{1-}^{1/2})$ dispersive calculations agree with the fit result, the result for $\text{Re} M_{1-}^{3/2}$ in Fig. 17 differs by a factor 2 from the theoretical results, which are essentially the Born terms. This result is surprising because one would expect deviations to occur in the isospin 1/2 - part (as P_{11} is inelastic above $E_\gamma = 400$ MeV) and not in the isospin 3/2 part (as P_{31} is elastic up to $E_\gamma \approx 800$ MeV).

A possible explanation could be the inclusion of ω -exchange in dispersive calculations which is known to change $M_{1-}^{3/2}$ substantially (Cp. ref. (41)). Unfortunately, when adding ω -change in the usual manner, cp. ref. (2, 5), one runs the risk of double counting⁽⁵⁾.

On the other hand, the result for this multipole from the iso-bar model^(6, 7) and the result of Walkers' analysis are in essential agreement to the fit result. But, for the isospin 1/2 part the two results of Berends and Donnachie (BD1, BD2 in Fig. 18) disagree completely with the result of Fig. 17 - note the factor 10^{-1} !

The result of the analysis for $\text{Re} E_{0+}^{3/2}$ in Fig. 19 shows larger error bars below resonance than above. This corresponds to the fact that below $E_\gamma = 340$ MeV no data exist for the π^0 differential cross sections at small pion CM angles. Accurate measurements for $\gamma p \rightarrow p\pi^0$ below $\theta_{CM} = 80^\circ$ are needed! Comparing Fig. 19 to the broad band of theoretical results and the results of other analyses, see Fig. 20, we observe a somewhat steeper slope of $\text{Re} E_{0+}^{3/2}$ in the fit result.

In Fig. 21 the result of the analysis for $E_{1+}^{3/2}$ is shown in an Argand diagram. Apart from the region near to threshold the result for this multipole lie fairly well on a circle. Strong evidence exist for a zero at $E_\gamma \approx 360$ MeV indicating a CDD zero also in this amplitude. In order to compare to the theoretical results, in Fig. 22, the ratio

$$E_{1+}^{(3/2)} / M_{1+}^{(3/2)}$$

is drawn. The fit result essentially agrees with that of the dispersive

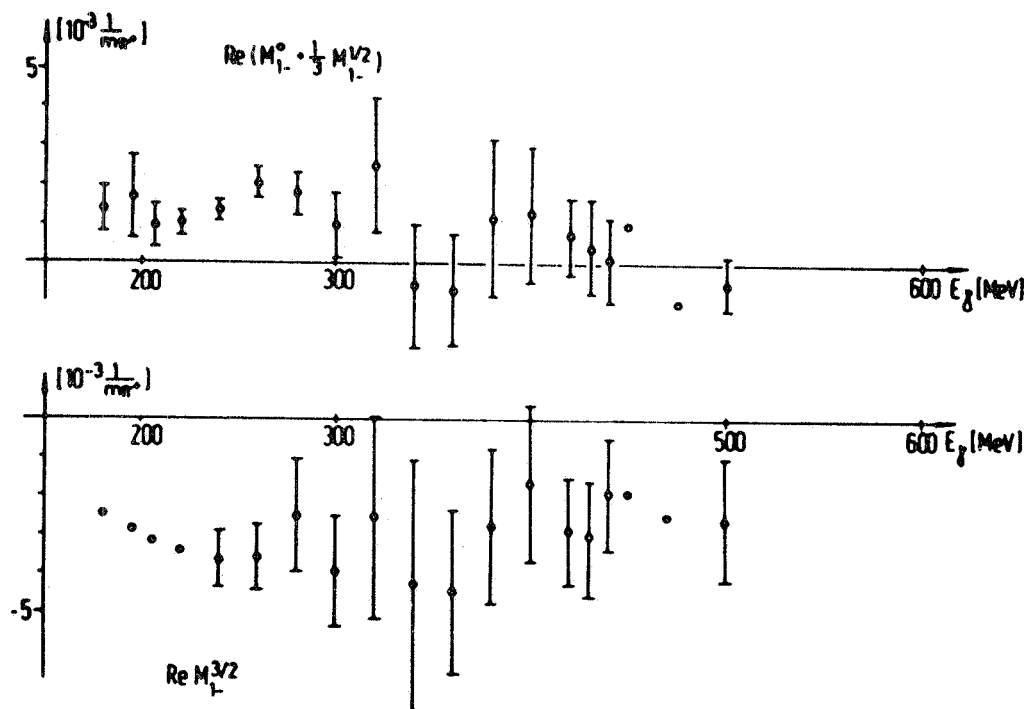


FIG. 17 - Result of the analysis for $\text{Re}(M_{1-}^0 + \frac{1}{3} M_{1-}^{1/2})$ - upper part - and for $\text{Re} M_{1-}^{3/2}$ - lower part.

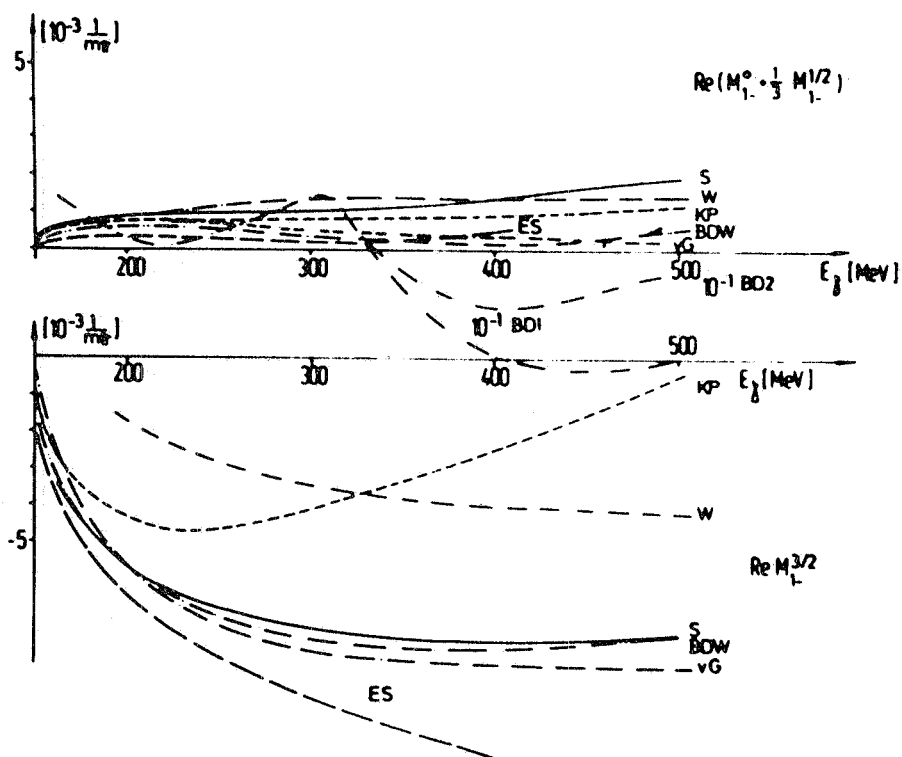


FIG. 18 - Results for M_{1-} from previous calculations. Notation as in Fig. 16.

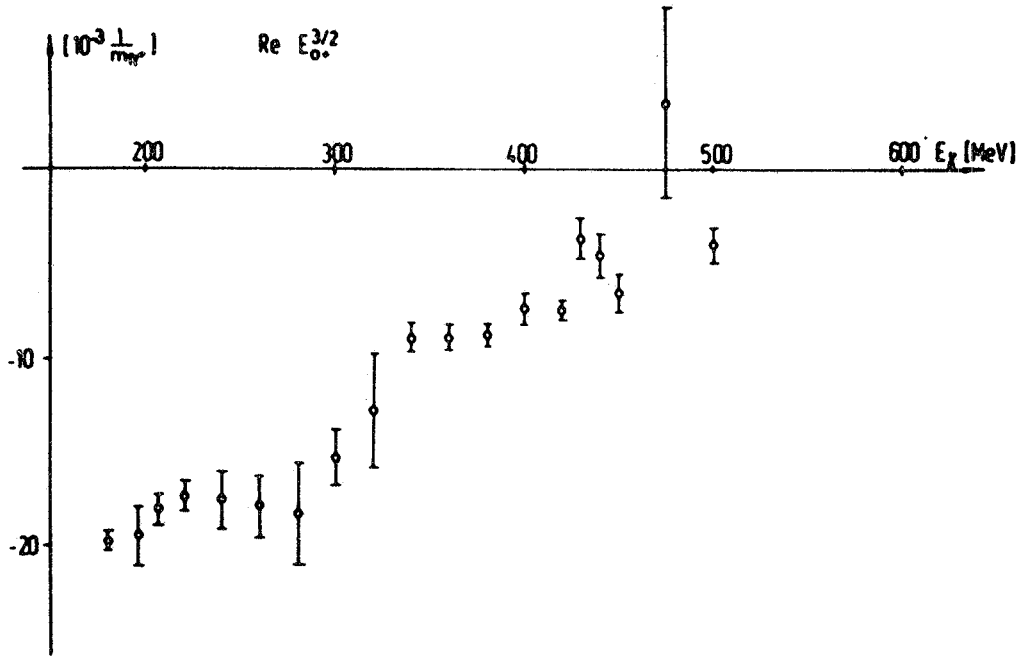


FIG. 19 - Result of the multipole analysis for $\text{Re } E_{0+}^{3/2}$.

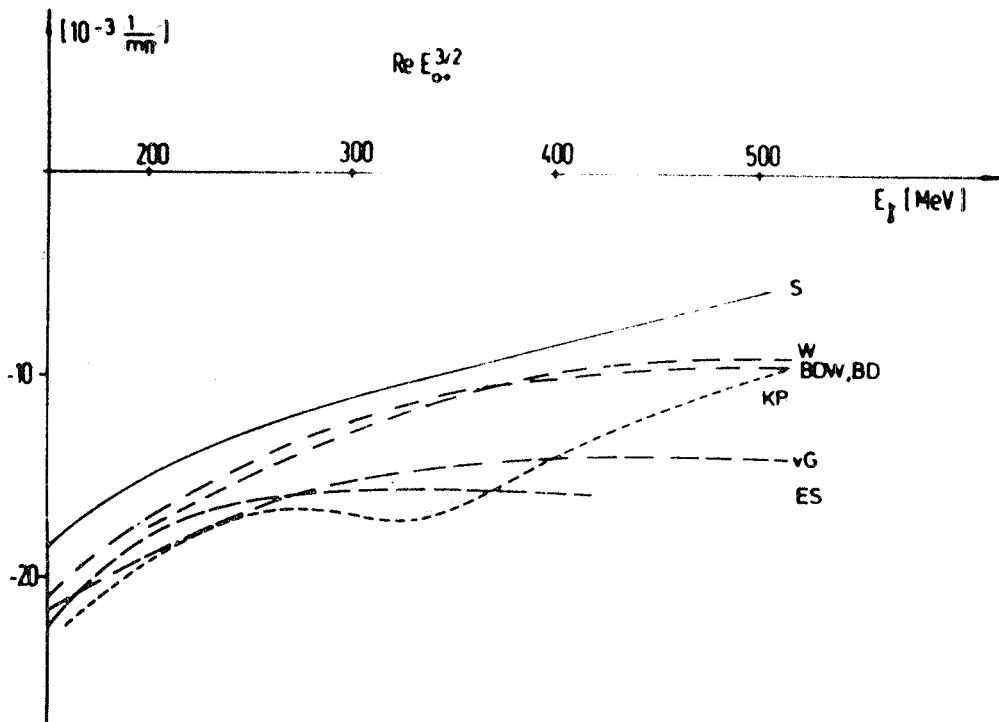


FIG. 20 - Previous results for $\text{Re } E_{0+}^{3/2}$.

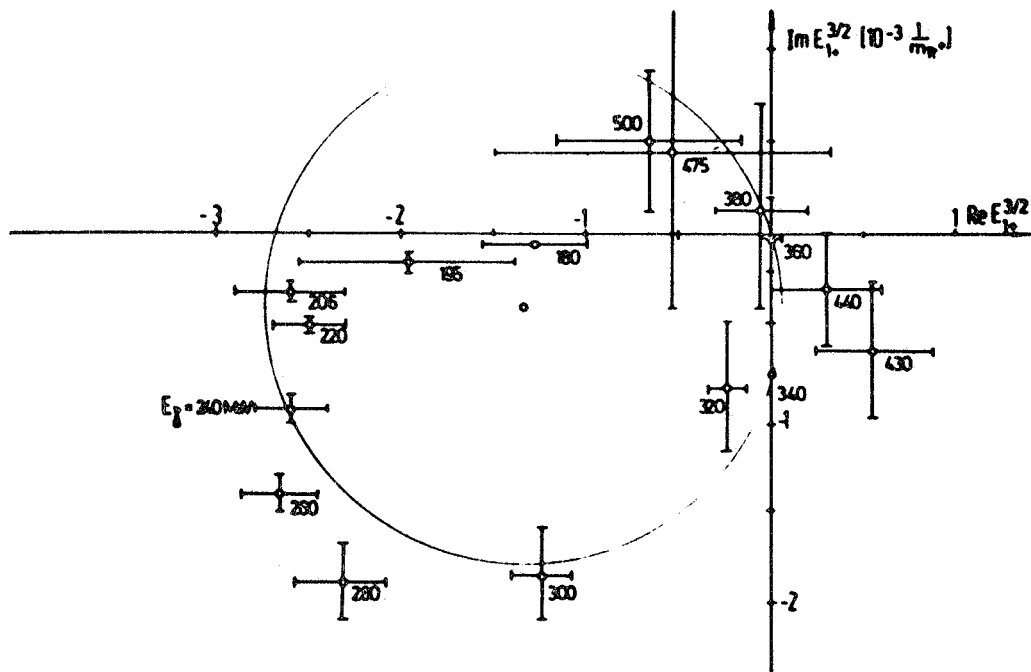


FIG. 21 - Argand plot for $E_{1+}^{3/2}$ from multipole analysis.

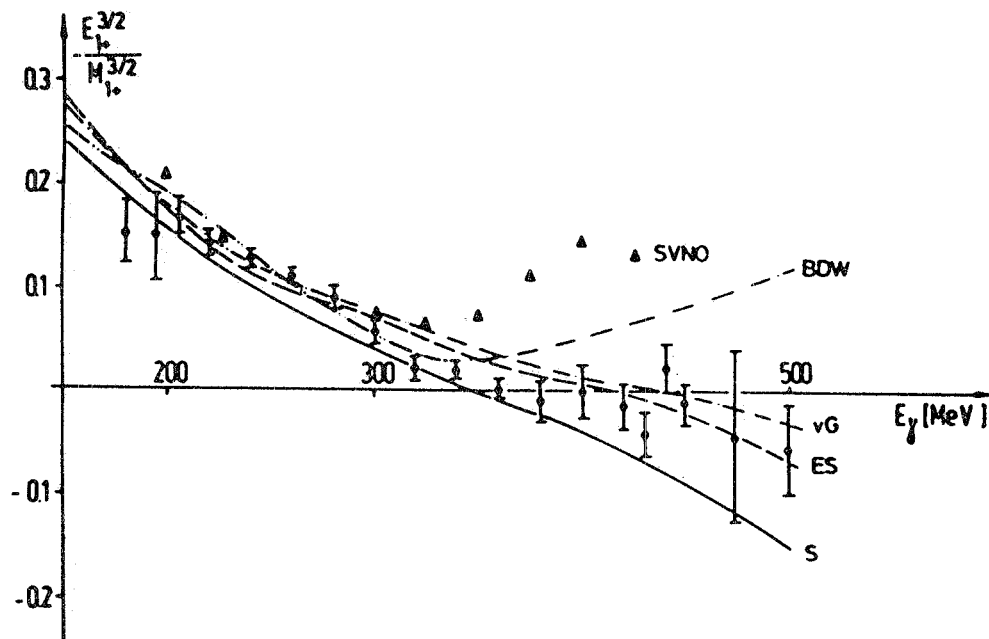


FIG. 22 - The ratio $E_{1+}^{3/2} / M_{1+}^{3/2}$ from analysis compared to several previous calculations.

calculations of von Gehlen⁽⁴⁾, Engels-Schmidt⁽³⁾ and Schwela^(5a) but disagrees with that of Berends, Donnachie and Weaver⁽²⁾. As for the analysis of Spillantini et al. ⁽³⁶⁾ the energy dependence of this ratio seems to be different but no definite conclusion can be drawn since the errors quoted in their paper are quite large.

To conclude this discussion, it is interesting to compare the results of the multipole analysis for

$$\text{Re } E_{0+}^{\pi^+}, \quad \text{Re } (E_{1+} - M_{1+})^{\pi^+} \quad \text{and} \quad \text{Re } (2 M_{1+} + M_{1-})^{\pi^+}$$

with the predictions from current density commutators obtained by Furlan, Paver and Verzegnassi⁽⁴²⁾. This is done in Table II. At three hold the agreement is excellent, above $E_\gamma = 220$ MeV some deviations occur in all three amplitudes which amount to at most 25% at the highest energy considered.

These are the essential results of the multipole analysis⁽³²⁾. For more details the diligent reader is referred to the original paper.

III. - SUMMARY OF RESULTS OF THE MULTIPOLE ANALYSIS. SUGGESTIONS FOR FURTHER EXPERIMENTS. -

- 1) In the multipole analysis of ref. (32) a consistent and satisfactory determination of the ($l \leq 1$) multipole amplitudes of single pion photoproduction on protons in the region of the first pion nucleon resonance has been obtained. Disregarding small jumps at resonance (cp. e. g. Fig. 19), the energy dependence of the multipoles obtained is very smooth. All data included in the analysis are very well fitted.
- 2) The magnetic dipole amplitude $M_{1+}^{3/2}$ shows impressively the Breit-Wigner shape of the P_{33} resonance in photoproduction.
- 3) For various multipoles the solution obtained differs significantly from the results of several theoretical calculations and of previous phenomenological multipole analysis. These discrepancies are particularly exhibited in $M_{1-}^{3/2}$ and - to a smaller extent - in $M_{1+}^{3/2}$ in the whole energy region covered. The isospin 1/2 parts of E_{1+} and M_{1+} , although very small, are well determined in the analysis. Both appear to have a zero at $E_\gamma \approx 450$ MeV, while theoretical calculations yield nearly constant values above resonance. The energy dependence of $E_{0+}^{3/2}$ turns out to be stronger than indicated in previous work.
- 4) The energy dependence of the multipoles above $E_\gamma = 440$ MeV is not established beyond any doubt. More data for the differential cross sections for $\gamma p \rightarrow p\pi^0$ are needed.

TABLE II

CA prediction				
E_γ (MeV)	$\text{Re}E_{0+}^{\pi^+}$	$\text{Re}(E_{1+}^{-M_{1+}})^{\pi^+}$	$\text{Re}(2M_{1+}^{+M_{1-}})^{\pi^+}$	
180	25.38	7.61	- 7.21	
200	24.07	10.97	- 10.39	
220	23.18	14.1	- 13.36	
240	22.26	17.1	- 16.21	
260	21.46	20.1	- 19.11	
Results of the multipole analysis				
E_γ (MeV)	$\text{Re}(E_{0+}^{\pm \Delta E_{0+}})^{\pi^+}$	$\text{Re}(E_{1+}^{-M_{1+}} \pm \Delta(E_{1+}^{-M_{1+}}))^{\pi^+}$	$\text{Re}(2M_{1+}^{+M_{1-}} \pm \Delta(2M_{1+}^{+M_{1-}}))^{\pi^+}$	
180	25.16 ± 0.37	6.67 ± 0.88	- 5.91 \pm 2.3	
200	22.10 ± 0.8	11.05 ± 0.82	- 13.15 \pm 2.4	
220	18.63 ± 0.57	14.07 ± 0.31	- 18.90 \pm 0.81	
240	18.13 ± 1.04	15.52 ± 0.48	- 21.30 \pm 1.13	
260	17.57 ± 1.05	16.64 ± 0.52	- 22.64 \pm 1.35	

Comparison of the results of the multipole analysis (32) with the results of current algebra (42). The multipoles are in units of $10^{-3} 1/m_\pi$. The errors quoted are absolute errors.

5) Suggestions for further experiments.

A) In order to reduce the error bars of various multipoles - in particular M_{1-} and E_{0+} below resonance - one should measure

$$\frac{d\sigma}{d\Omega} (\gamma p \rightarrow p\pi^0) \quad \text{for} \quad \theta_{CM} \leq 80^\circ$$

$$E_\gamma \leq 340 \text{ MeV}$$

angular distributions of the asymmetry ratio $\Sigma(\theta)$ for $\gamma p \rightarrow p\pi^0$

angular distributions of the recoil nucleon polarization $P(\theta)$ for $\gamma p \rightarrow p\pi^0$.

In order to distinguish between solution A and solution B the polarized target asymmetry $\Xi(\theta)$, defined in eq. (8), should be measured at pion CM angles below $\pi/2$.

B) In order to allow a complete multipole analysis, i. e. a separation of isoscalar and isovector - 1/2 - terms, data on the process

$$(9) \quad \gamma n \rightarrow p\pi^-$$

are required.

Angular distribution of differential cross sections should be measured from an investigation of the inverse reaction which avoids the spectator model.

But also data on the π^-/π^+ -ratio on deuterons

$$(10) \quad R_d^{\pi^\pm} = \frac{\frac{d\sigma}{d\Omega}(\gamma d \rightarrow pp_S \pi^-)}{\frac{d\sigma}{d\Omega}(\gamma d \rightarrow nn_S \pi^+)} \approx \frac{\frac{d\sigma}{d\Omega}(\gamma n \rightarrow p\pi^-)}{\frac{d\sigma}{d\Omega}(\gamma p \rightarrow n\pi^+)}$$

are very useful, which are reduced to free-nucleon-data by the spectator model. In the ratio the application of the spectator model will not be so critical as in absolute cross sections, as nuclear effects are expected to cancel out. Also the systematical errors^{of} such an experiments will be smaller.

For the same reason, also data on the asymmetry ratio for polarized photons are valuable.

Finally, all isotopic spin parts being determined, by such a complete multipole analysis, predictions for

$$(11) \quad \gamma n \rightarrow n\pi^0$$

can be made, which are to be compared to the data extracted from the π^0 photoproduction on nuclei (if one succeeds in establishing the validity of the impulse approximation). This comparison could help to decide the question of the existence of an isotensor current in electromagnetic interactions⁽⁴³⁾.

C) It is wanted to extend this kind of multipole analysis to higher energies (0.5 - 1.5 GeV). This would be valuable for a test of FESR and duality concepts in photoproduction. However, considering such an analysis, one has to be aware of the following facts :

- a) above $E_\gamma \approx 500$ MeV the Watson theorem breaks down for many multipoles - this boils down to a doubling of the parameters to be determined from experiment ;
- b) more multipole amplitudes contribute ;
- c) more channels are open.

For these reasons the analysis becomes much more involved and one needs many accurate data on quantities, in which interference terms play a large role, i. e.

$$\Sigma(\theta), \quad P(\theta) \quad \text{and} \quad \Xi(\theta)$$

and angular distributions of these quantities for $\gamma p \rightarrow p\pi^0$, $\gamma p \rightarrow n\pi^+$ and $\gamma n \rightarrow p\pi^-$ are necessary.

Moreover, the gap in the data for the differential cross sections of the photoproduction on protons between $E_\gamma = 450$ and 600 MeV should be filled. Also the discrepancies observed in the cross section data above $E_\gamma = 600$ MeV (cp. e.g. Fig. 3) are to be resolved by the experimentalists. Before this experimental program is done, no decisive progress will be obtained in understanding pion photoproduction between 0.5 and 1.5 GeV and any multipole analysis will need a lot of assumptions which are not on a sure footing.

REFERENCES. -

- (1) - G. F. Chew, M. L. Goldberger, F. E. Low and J. Nambu (referred to as CGLN), Phys. Rev. 106, 1345 (1957).
 (2) - F. A. Berends, A. Donnachie and D. Weaver (BDW), Nuclear Phys. B4, 1, 54, 103 (1969).
 (3) - J. Engels and W. Schmidt (ES), Phys. Rev. 169, 1296 (1968); J. Engels, A. Müllensiefen and W. Schmidt, Phys. Rev. 175, 1951 (1968).
 (4) - G. von Gehlen (vG), Nuclear Phys. B20, 102 (1970).
 (5) - D. Schwela and R. Weizel, Z. Physik 221, 71 (1969); D. Schwela, H. Rollnik, R. Weizel and W. Korth, Z. Physik 202, 451 (1967).
 (5a) - D. Schwela (S), unpublished calculations; these calculations repeat those of ref. (5) using the new Bonn data^(12, 14) for the determination of the parameters. Actually, from the proton differential cross section data four parameters out of six have been determined, viz. for

$$\begin{array}{cccc}
 M_{1+}^{3/2} & E_{1+}^{3/2} & E_{0+}^0 + \frac{1}{3} E_{0+}^{1/2} & M_{1-}^0 + \frac{1}{3} M_{1-}^{1/2} \\
 C_{M_{1+}^{3/2}} & C_{E_{1+}^{3/2}} & C_{E_{0+}^+} & C_{M_{1-}^+}
 \end{array}$$

The remaining two for

$$\begin{array}{cc}
 E_{0+}^0 - \frac{1}{3} E_{0+}^{1/2} & M_{1-}^0 - \frac{1}{3} M_{1-}^{1/2} \\
 C_{E_{0+}^-} & C_{M_{1-}^-}
 \end{array}$$

had to be determined from data for $\gamma n \rightarrow p\pi^-$, see ref. (28).

- (6) - Kim Yong Taik (KP), Diplomarbeit, Bonn (1968).
 (7) - W. Pfeil (KP), Ph.D. Thesis, Bonn (1968); to be published.
 (8) - K. M. Watson, Phys. Rev. 95, 228 (1954).
 (9) - L. Castillejo, R. H. Dalitz and F. J. Dyson, Phys. Rev. 101, 453 (1956).
 (10) - H. Rollnik, in "Proc. Heidelberg Intern. Conf. on Elementary Particles (1967)" p. 400; in "Methods in subnuclear physics, edited by M. Nikolic (1968)", vol. III, p. 666 ff.
 (11) - D. L. Weaver, Lectures held at the Laboratori Nazionali del CNEN, Frascati, LNF-69/69 (1969).
 (12a) - G. Fischer, H. Fischer, G. von Holtey, H. Kämpgen, G. Knop, P. Schutz, H. Wessels, W. Braunschweig, H. Genzel and R. Woldemeyer, Nuclear Phys. B16, 93 (1970).
 (12b) - R. Morand, E. F. Erickson, J. P. Pahin and M. G. Croissiaux, Phys. Rev. 180, 1299 (1969).
 (12c) - E. Hilger, H. Roegler and M. Tonutti, Contribution to the Kiev Conference.

- (13) - For the olders data see : J. T. Beale, S. D. Ecklund and R. L. Walker, Calthec report CTSL-42 (1966).
- (14a) - G. Fischer, H. Fischer, M. Henel, G. von Holtey, G. Knopf and J. Stümpfig, Nuclear Phys. B16, 119 (1970).
- (14b) - J. Bizot, J. P. Perez-Y-Jorba and D. Trulle, Phys. Letters 25B, 489 (1969).
- (15) - W. Hitzeroth, Nuovo Cimento 60, 467 (1969).
- (16) - B. B. Govorkov, S. P. Denisov and E. V. Minarik, Soviet J. Nuclear Phys. 6, 370 (1968).
- (17a) - G. Barbiellini, G. Bologna, G. Capon, G. de Zorzi, F. L. Fabbri, G. P. Murtas, G. Sette, G. Diambri and J. de Wire, Phys. Rev. 184, 1402 (1969).
- (17b) - D. J. Drickey and R. F. Mozley, Phys. Rev. 136, B 543 (1964).
- (17c) - G. Bologna, F. L. Fabbri, P. Spillantini and V. Valente, Frascati report LNF-70/39 (1970).
- (18) - See : R. L. Walker, Proc. 4th Intern. Symp. on Electron and Photon Interactions, Liverpool (1969), p. 23.
- (19) - Aachen-Berlin-Bonn-Hamburg-Heidelberg-München Collaboration, Nuclear Phys. B8, 539 (1968).
- (20) - J. Favier, J. C. Alder, C. Joseph, B. Vaucher, D. Schnizel, C. Zupancic, T. Bressani and E. Chiavassa, Phys. Letters 31B, 609 (1970).
- (21) - D. Schnizel, private communication, has obtained some changes in the data of ref. (10), when repeating the calculations.
- (22) - F. Carbonara et al., Lettere Nuovo Cimento 3, 697 (1970).
- (23) - T. Nishikawa et al., Phys. Rev. Letters 21, 1288 (1969).
- (24) - F. F. Liu, D. J. Drickey and R. F. Mozley, Phys. Rev. 136, B 1183 (1964).
- (25) - P. A. Berardo et al., Phys. Rev. Letters 24, 419 (1970).
- (26) - G. Gatti et al., Phys. Rev. Letters 6, 706 (1961).
- (27) - P. Gorenstein et al., Phys. Letters 19, 157 (1965); Phys. Letters 23, 394 (1966); M. Grilli et al., Frascati report LNF-67/18 (1967).
- (28) - D. Schwela, Z. Physik 221, 158 (1969).
- (29) - M. Gourdin and P. Salin, Nuovo Cimento 27, 193, 309 (1963); P. Salin, Nuovo Cimento 28, 1294 (1963); Nuovo Cimento 32, 521 (1964).
- (30) - A. M. Harun-ar-Rashid and M. J. Moravscik, Ann. Phys. 35, 331 (1965); J. P. Loubaton, Nuovo Cimento 39, 591 (1965); H. Shimoda, Y. Sumi and H. Jakomi, Prog. Theoret. Phys. 37, 1167 (1967).
- (31) - H. De Staebler Jr., E. F. Erickson, A. C. Hearn and C. Schaerf, Phys. Rev. 140, 336 (1965).
- (32) - P. Nölle, W. Pfeil and D. Schwela, Nuclear Phys., to be published.
- (33) - F. A. Berends and A. Donnachie (BD, BD1, BD2), University of Glasgow preprint; 4th Intern. Symp. on Electron and Photon Interactions at High Energies, Liverpool (1969), Contr. N^o. 140.

- (34) - R. L. Walker (W), Phys. Rev. 182, 1729 (1969).
- (35) - M. Grilli, P. Spillantini, V. Valente and E. Schiavuta, Nuovo Ci-mento 68, 1189 (1969).
- (36) - P. Spillantini, V. Valente, M. Nigro and C. Oleari (SVNO), Nu-clear Phys. B13, 320 (1969).
- (37) - Y. M. Aleksandrov, V. F. Grushin and E. M. Leikin, Lebedev Institute preprint n. 46 (1970).
- (38) - A. Müllensiefen, Z. Physik 211, 360 (1968).
- (39) - T. Wennström, Nuclear Phys. B5, 235 (1968).
- (40) - K. Kondo, T. Nishikawa, T. Suzuki and K. Takikawa, J. Phys. Soc. Japan 29, 30 (1970).
- (41) - See the results for $\Sigma(90^\circ)$ quoted by: H. Rollnik, Heidelberg Intern. Conf. on Elementary Particles (1967), ref. (10).
- (42) - G. Furlan, N. Paver and C. Verzegnassi, Trieste preprint IC/70/27 (1970); C. Verzegnassi, private communication.
- (43) - D. Schwela, Nuclear Phys., to be published.